

# Physicochemical Properties and Skin Protection Activities of Polysaccharides from *Usnea longissima* by Graded Ethanol Precipitation

Ziying Yang,<sup>1</sup> Yajie Hu,<sup>1</sup> Panpan Yue, Hongdan Luo, Qisui Li, Huiling Li, Zhang Zhang, and Feng Peng\*



Cite This: *ACS Omega* 2021, 6, 25010–25018



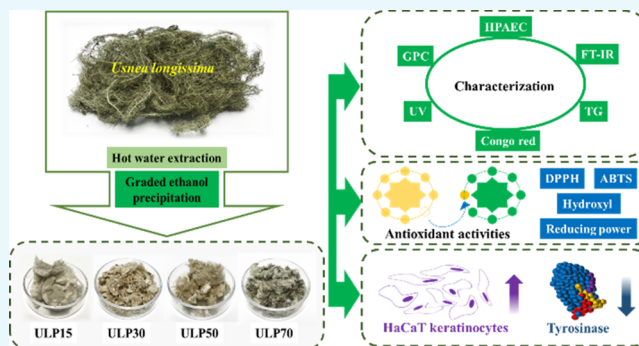
Read Online

ACCESS |

Metrics & More

Article Recommendations

**ABSTRACT:** Four *Usnea longissima* polysaccharides (ULPs; ULP15, ULP30, ULP50, and ULP70) were obtained from the lichen *U. longissima* via water extraction and graded ethanol precipitation. The obtained ULPs were all heteropolysaccharides with a few proteins, with which glucose was the major monosaccharide composition. With the increase in the precipitated ethanol concentrations, the content of galactose, xylose, and mannose increased, whereas that of glucose decreased. Moreover, the antioxidant activity test demonstrated that ULP15 exhibited better reducing power and stronger scavenging ability on 2,2-diphenyl-1-picrylhydrazyl (DPPH) and hydroxyl free radicals. Importantly, ULP15 also had a better proliferative effect on human HaCaT keratinocytes and dermal fibroblasts. Meanwhile, ULP15 protected HaCaT keratinocytes from UVB-induced proliferation inhibition and exhibited tyrosinase inhibition activity. Therefore, this work provides interesting insight into the preparation of cosmetic ingredients using the polysaccharide ULP15.



## 1. INTRODUCTION

Skin is directly exposed to environmental stimuli like solar radiation from the sun, which will result in oxidative stress and skin disorders due to UVB (ultraviolet B) radiation. Oxidative stress could reduce antioxidant enzyme activity and increase intracellular reactive oxygen species (ROS) levels. The intracellular ROS accumulation will not only lead to photoaging reactions but also stimulate the activity of tyrosinase.<sup>1</sup> As a copper-containing monooxygenase, tyrosinase plays a key role in catalyzing the physiological process of melanin synthesis.<sup>2</sup> The stimulating effects on tyrosinase will result in aberrant melanin production, which brings about dark spots, freckles, and hyperpigmentation.<sup>3</sup> Hyperpigmentation, including melasma, freckles, and leukoplakia, can be a serious aesthetic problem, which is caused by the abnormal accumulation of melanin pigments.<sup>4</sup> Therefore, the inhibition of tyrosinase activity is a crucial factor in preventing hyperpigmentation. In addition, free radical scavengers or antioxidants can also effectively suppress hyperpigmentation. Hence, natural bioactive resources with antityrosinase and antioxidant activity have attracted more interest in inhibiting melanin synthesis and hyperpigmentation.

Natural polysaccharides are significant bioactive macromolecule resources with biocompatibility, cost-effectiveness, and low toxicity that possess a variety of biological activities,

including antioxidant, antibacterial, antiviral, anti-inflammatory, anticoagulant, and antitumor activities.<sup>5</sup> Of course, polysaccharides have also been considered as prospective resources for preventing hyperpigmentation and maintaining the skin.<sup>4,6</sup> Previous reports indicated that *Sargassum siliquastrum* polysaccharides can protect keratinocytes from UVB-induced injury by attenuating ROS levels and suppressing mitochondria-mediated apoptosis,<sup>7</sup> aloe polysaccharides can not only improve cell viability and proliferation but also protect skin nerve cells from UVB-induced injury,<sup>8</sup> and *Pholiota nameko* polysaccharides have good moisture-preserving and antioxidant activities.<sup>9</sup> However, a few works were devoted to the application of lichen polysaccharides in skincare.

Lichens are formed by the symbiotic association of fungi and algae (or cyanobacterium) and produce a wide array of both primary and secondary metabolites.<sup>10</sup> The main components

Received: August 4, 2021

Accepted: September 8, 2021

Published: September 16, 2021

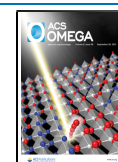


Table 1. Yield and Chemical Composition of ULPs

index	sample			
	ULP15	ULP30	ULP50	ULP70
yield <sup>a</sup> (% w/w)	1.60 ± 0.00	0.52 ± 0.00	1.83 ± 0.00	1.22 ± 0.00
carbohydrate (% w/w)	73.84 ± 0.48	77.11 ± 0.30	71.68 ± 0.46	75.09 ± 0.66
protein (% w/w)	2.56 ± 0.15	2.63 ± 0.06	1.81 ± 0.16	2.41 ± 0.05

<sup>a</sup>Based on eq 1.

Table 2. Physicochemical Properties of ULPs

sample	monosaccharide composition <sup>a</sup> (molar ratio, mol %)					molecular weight <sup>b</sup>				
	Ara	Gal	Glu	Xyl	Man	GalA	GluA	$M_w$	$M_n$	$M_w/M_n$
ULP15	1.07	8.62	78.96	0.66	13.27	1.19	1.23	76,400	61,990	1.23
ULP30	ND	11.47	69.54	0.97	14.75	1.72	1.55	39,000	21,680	1.80
ULP50	ND	12.86	54.44	1.2	26.93	1.51	3.06	126,000	71,950	1.75
ULP70	4.79	20.42	39.09	4.51	27.37	1.29	2.53	59,200	26,830	2.21

<sup>a</sup>Ara, arabinose; Gal, galactose; Glc, glucose; Xyl, xylose; Man, mannose; GalA, galacturonic acid; GluA, glucuronic acid; ND, not detected. <sup>b</sup> $M_w$ , weight-average molecular weight;  $M_n$ , number-average molecular weight;  $M_w/M_n$ , polydispersity index.

of primary metabolites are polysaccharides, which are generally considered to be of fungal origin, including  $\alpha$ -glucans,  $\beta$ -glucans, and galactomannans.<sup>11</sup> In the past five decades, much research has been performed to show the antitumor and immunomodulatory biological activity of lichen polysaccharides with a low toxicity level.<sup>12</sup> However, lichen polysaccharides as active entities in cosmetic ingredient preparation are not commonly described. *Usnea longissima* (*U. longissima*) is a common and widely distributed lichen species. The first known recorded use of *U. longissima* can be traced back to 101 B.C., while it was used in the treatment of external ulcers, asthma, tuberculosis, and fever in the form of wound dressing or decoction. Previously, various studies focused on *U. longissima* to explore its secondary metabolites.<sup>13</sup> To the best of our knowledge, the physicochemical properties and biological activities of the graded ethanol-fractionated *U. longissima* polysaccharides were not reported.

In this work, the hot water-extracted *U. longissima* polysaccharides (ULPs) were fractionated and purified by graded precipitation at ethanol concentrations of 15, 30, 50, and 70% (v/v). Furthermore, the physicochemical properties, antioxidant activities, and skin-protective activities in vitro of the purified ULPs were also investigated, indicating that ULPs could be a new and excellent cosmetic ingredient.

## 2. RESULTS AND DISCUSSION

**2.1. The Yield and Chemical Composition of ULPs (ULP15, ULP30, ULP50, and ULP70).** The yield and chemical composition of ULPs are summarized in Table 1. ULP50 has the highest yield value of 1.83% and is followed by ULP15 with a yield of 1.60%, which suggested that ULP50 and ULP15 are the main components of ULPs. Additionally, carbohydrate and protein contents of ULPs were also detected. Among them, ULP30 contained the highest contents of carbohydrates (77.11 ± 0.30%), as well as the maximum amount of protein (2.63 ± 0.06%). Compared with polysaccharides with skin protection ability in the previous reports,<sup>3,14</sup> ULPs had higher carbohydrate content but lower protein content, which suggested that ULPs exhibited less protein contamination and better skin protection ability.

**2.2. Monosaccharide Compositions of ULPs.** The monosaccharide compositions of ULPs are summarized in

Table 2. The glucose in ULPs was the major monosaccharide, followed by mannose and galactose. However, arabinose, xylose, galacturonic acid, and glucuronic acid were just a small quantity. The existence of uronic acid, combined with the protein detected in Section 2.1, suggests that ULPs are acidic proteoglycans. As the ethanol concentration increased, the content of glucose in the ULPs decreased, while the content of galactose and mannose in ULPs increased. Specifically, ULP15 exhibited the highest glucose content, and ULP70 exhibited the highest galactose, xylose, and mannose content.

**2.3. Molecular Weight Distribution of ULPs.** The average weight molecular weight ( $M_w$ ) and number average molecular weight ( $M_n$ ) of ULPs were determined. As shown in Table 2, the  $M_w$  values of ULPs were 76,400, 39,000, 126,000, and 59,200, respectively. Among them, ULP50 exhibited the highest  $M_w$  and ULP30 exhibited the lowest  $M_w$ . Furthermore, the polydispersity indices (1.23–2.21) indicated a relatively narrow molecular weight distribution of ULPs. These results showed that  $M_w$  is associated with the ethanol concentration, and graded ethanol precipitation is a reliable and efficient method to fractionate polysaccharides with different  $M_w$  values from *U. longissima*.

**2.4. Nucleic Acid and Protein Analysis of ULPs.** The existence of nucleic acid and protein was detected by ultraviolet–visible (UV–Vis) spectroscopy. As shown in Figure 1, two obvious absorption peaks appeared at the wavelengths of 260 and 280 nm in the UV spectra of ULPs,

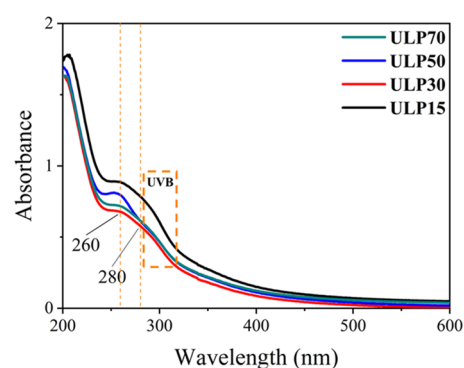


Figure 1. UV spectra of ULPs.

which represent the existence of nucleic acid and protein.<sup>15</sup> In addition, absorbance signals at 290–320 nm also existed in the UV spectra of ULPs, which is the UVB range. From these results, it can be speculated that ULPs probably exhibited skin protection ability by absorbing solar UVB radiation and preventing deeper penetration and damage.<sup>16</sup>

**2.5. Structure Analysis.** Fourier-transform infrared spectroscopy (FT-IR) spectra were used to detect the chemical structure of ULPs, and the results are shown in Figure 2. In

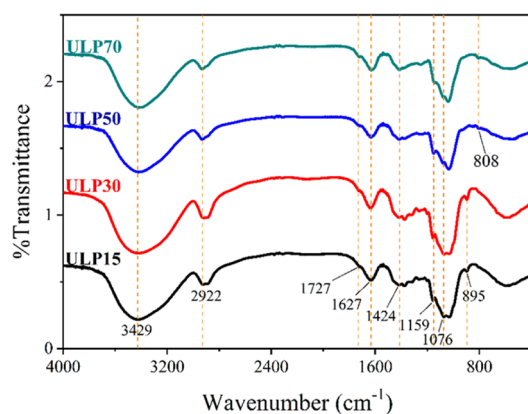


Figure 2. FT-IR spectra of ULPs.

general, the FT-IR spectra of the ULPs were almost identical. The strong bands at 3429 and 2922  $\text{cm}^{-1}$  both belonged to the characteristic functional groups of polysaccharides.<sup>17</sup> The bands at 1727 and 1627  $\text{cm}^{-1}$  suggest the C=O stretching vibrations of esters and the asymmetric stretching vibration of carboxylate anions ( $\text{COO}^-$ ),<sup>18</sup> respectively, which indicates that all obtained ULPs contained uronic acid. The absorption band at 1424  $\text{cm}^{-1}$  is associated with the variable angle vibration of the N–H group, which indicated the existence of the protein.<sup>19</sup> The presence of uronic acids and proteins was consistent with the results of monosaccharide composition and chemical composition analyses. In addition, the absorption peaks in the range of 1200–800  $\text{cm}^{-1}$  are considered as the “fingerprint” of polysaccharides, among which the absorptions at 1159 and 1076  $\text{cm}^{-1}$  indicate the presence of the pyranose,<sup>20</sup> the absorptions at 895  $\text{cm}^{-1}$  arise from the presence of  $\beta$ -pyranose, and the bands at 808  $\text{cm}^{-1}$  suggest the presence of  $\alpha$ -pyranose.<sup>21</sup> By comparing the “fingerprint” in the FT-IR spectra of ULPs,  $\beta$ -pyranose appeared in ULP15 and ULP30, yet  $\alpha$ -pyranose appeared in ULP50 and ULP70. These results suggested that ULPs all contained hydroxyl, ester, amino, alkyl, and carboxyl, which will contribute to the field of antioxidant and skin protection activities of ULPs.

The triple helix structure of ULPs was determined by Congo red test. Generally speaking, polysaccharides with helical conformation can connect with Congo red to form a stable complex, which results in a redshift of Congo red at the maximum absorption wavelength ( $\lambda_{\text{max}}$ ).<sup>22</sup> As shown in Figure 3, the  $\lambda_{\text{max}}$  of ULP–Congo red complexes exhibited a blueshift trend at weakly alkaline solutions and then stabilization with increasing NaOH concentrations, which demonstrated that the ULPs had no triple-helical conformation in the solution.

**2.6. Thermogravimetric Analysis of ULPs.** The thermal stability of ULPs is an important characteristic considered for cosmetics industry applications. The thermostability of ULPs was evaluated using thermogravimetry (TG) and differential

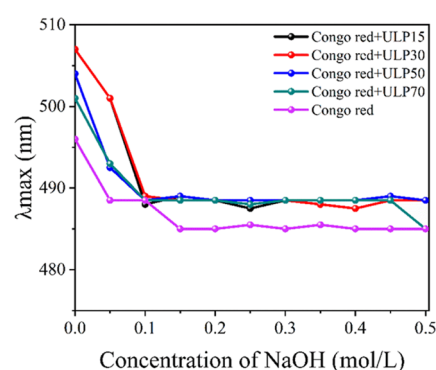
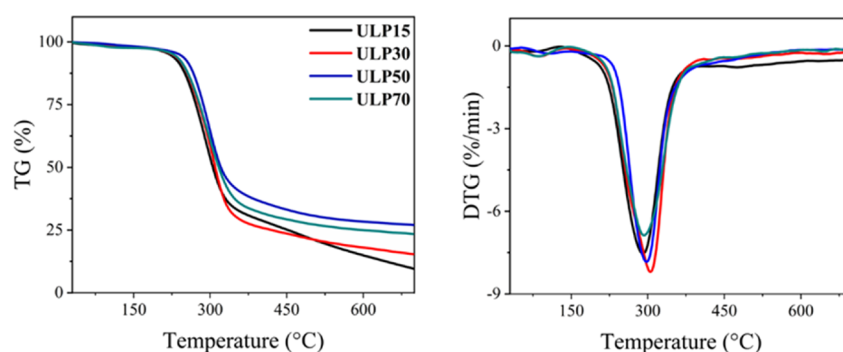


Figure 3.  $\lambda_{\text{max}}$  of Congo red, Congo red + ULP15, Congo red + ULP30, Congo red + ULP50, and Congo red + ULP70 at various concentrations of sodium hydroxide solution.

thermogravimetry (DTG). As shown in Figure 4, the very small initial weight loss of ULPs occurred between 26 and 142  $^{\circ}\text{C}$  and the weight loss was approximately 1.8%, which was likely attributed to the vaporization of the absorbent and structural water of the polysaccharide.<sup>23</sup> The second weight loss process appeared at about 230–340  $^{\circ}\text{C}$ , and ULPs showed a sharp mass loss with an overall weight loss of at least 48.8%. The results indicated the violent decomposition of ULPs, which was probably attributed to the cleavage of the carbon chain and hydrogen bonds.<sup>24</sup> In addition, no obvious peak was observed after 350  $^{\circ}\text{C}$ , which corresponded to ULPs having higher carbohydrate content but lower protein content.<sup>25</sup>

**2.7. In Vitro Antioxidant Activity of ULPs.** As a well-qualitative and stable free radical, 2,2-diphenyl-1-picrylhydrazyl (DPPH) has been widely applied to the determination of the antioxidant abilities of natural products.<sup>19</sup> The DPPH free radical scavenging activities of ULPs are shown in Figure 5A. The DPPH radical scavenging activities increased with increasing ULP concentration. At 5 mg/mL, ULP15 showed the highest scavenging activity (66.98%) against DPPH free radicals. Moreover, the half inhibition concentration ( $\text{IC}_{50}$ ) values of ULP15, ULP30, ULP50, and ULP70 were 3.38, 4.70, 13.57, and 4.65 mg/mL, respectively. From the discussion so far, ULP15 exhibited better DPPH scavenging ability than those of other groups. According to previous reports, the antioxidant ability of polysaccharides in vitro might be associated with the existence of reducing sugar.<sup>26</sup> The effect of antioxidants on DPPH radical scavenging was conceived to be due to their proton-donating ability.<sup>27</sup> During the DPPH free radical scavenging period of ULPs, a gradual color change from purple to lavender was observed, which proved that ULPs could donate the hydrogen atoms that can reduce the DPPH radical to DPPH-H. As a result, ULPs showed certain antioxidant activity, which could be used in the skin protection area.

A 2,2'-azinobis(3-ethylbenzothiazoline-6-sulfonic acid) ammonium salt (ABTS) radical cation has also been used to evaluate the antioxidant activity of natural plant polysaccharides by using the spectrophotometric method.<sup>28</sup> The ABTS<sup>+</sup> scavenging abilities of ULPs are shown in Figure 5B. Within the tested dosage range (1–5 mg/mL), it was observed that the antioxidant activities of ULPs exhibited a concentration-dependent relationship. At 5 mg/mL, the maximum scavenging activity of 54.61% was reached by ULP70, while the scavenging effect of ascorbic acid (Vc) was 96.37%. The results suggested that ULPs could act as electron donors and react with ABTS<sup>+</sup>



**Figure 4.** TG and DTG curves of ULPs at a heating rate of 10 °C/min under a nitrogen atmosphere.

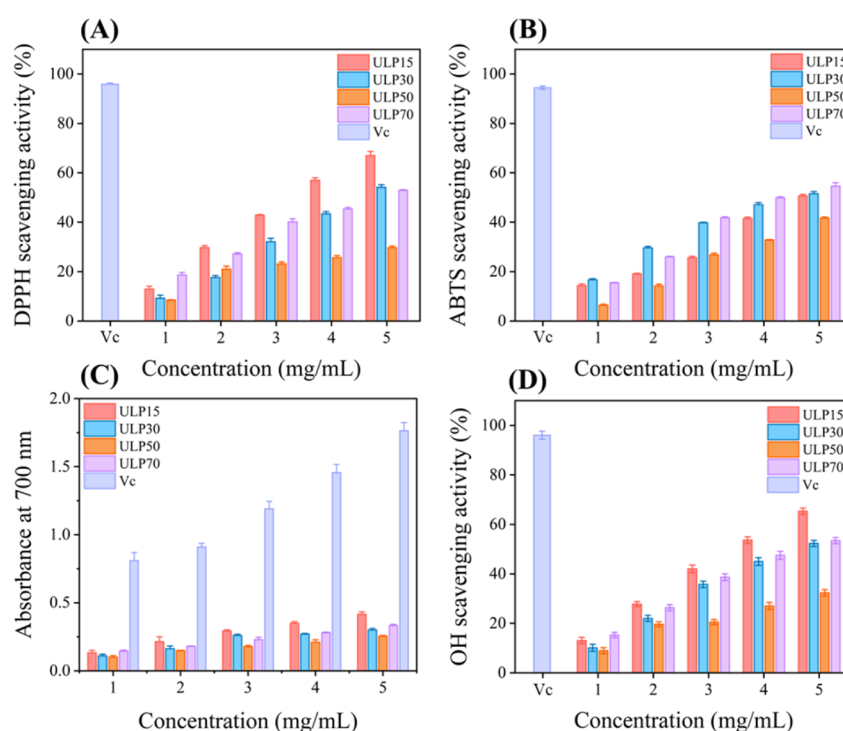


**Figure 5.** Antioxidant activities of ULPs. Vc (1 mg/mL) was a positive control. (A) DPPH radical scavenging activity; (B) ABTS radical scavenging activity; (C) reducing power of ULPs; (D) hydroxyl radical scavenging activity.

to terminate radical chain reactions. Compared with the other ULPs, the  $IC_{50}$  of ULP70 was about 4.17 mg/mL, which has the best scavenging ability. Some correlations could be observed between the ABTS radical scavenging activity and the physicochemical properties of ULPs by comparing with the results in Table 1. Previous research had demonstrated that the antioxidant activity of polysaccharides was associated with the contents of arabinose.<sup>22</sup> The arabinose content of ULP70 was higher than those of the other three ULPs, which makes a reasonable explanation for the highest antioxidant activity of ULP70. In addition, the molecular weight of polysaccharides was another key factor for their antioxidant abilities, and the higher molecular weight likely decreased their ability to provide reductive  $-OH$  terminals available for reacting with the radical series,<sup>29</sup> which might explain why ULP50 had the lowest radical scavenging activity in DPPH and ABTS.

The ferric reducing power was used to evaluate the antioxidant ability of the polysaccharides, since polysaccharides could generate the reduction of  $[Fe(CN)_6]^{3-}$  to  $[Fe(CN)_6]^{4-}$  by donating an electron. This reaction produced Prussian blue,

which had a maximum absorbance at 700 nm. Therefore, the absorbance values at 700 nm could reflect the reducing power of polysaccharides. As shown in Figure 5C, the reducing power of ULPs increased with increasing concentrations. At 5 mg/mL, the absorbance values of ULP15, ULP30, ULP50, ULP70, and Vc were determined to be 0.42, 0.3, 0.25, 0.33, and 1.76, respectively. ULP15 exhibited higher reducing power among the four ULPs. These observations might be ascribed to a more reducing end group of ULP15.

The ROS, including superoxide, hydroxyl, and singlet oxygen, occurred during the normal cellular metabolism of living organisms, and excessive levels may lead to metabolic disorders and accelerate cellular death.<sup>30–32</sup> Hydroxyl radicals are considered the most active free radicals among the ROS.<sup>33</sup> Therefore, removing hydroxyl radicals is quite significant for maintaining a balance between oxidative stress and antioxidant protection. As illustrated in Figure 5D, a positive correlation between the concentration and the scavenging hydroxyl radical rate of ULPs was observed in the whole tested concentration range (1–5 mg/mL). Meanwhile, ULP15 had the strongest



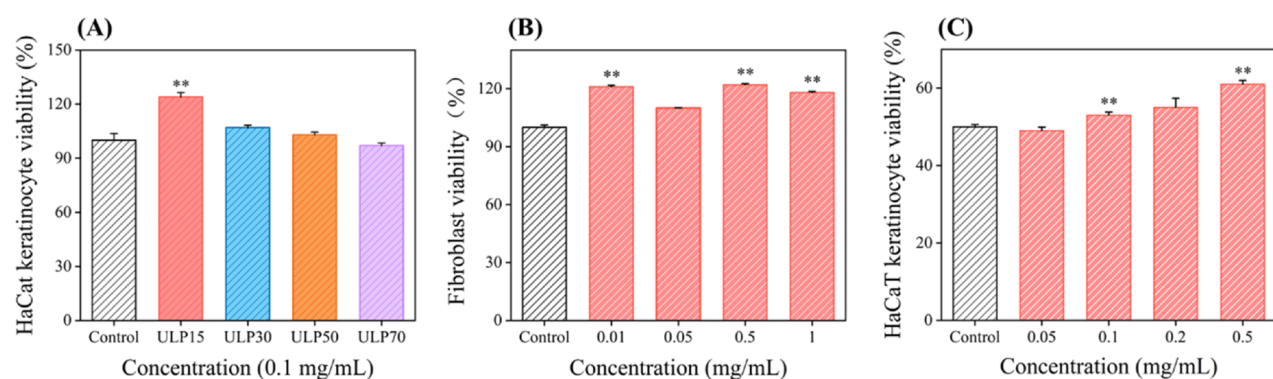


**Figure 6.** Proliferative effects on HaCaT keratinocytes and fibroblast cells and UVB-protective effects of ULP15 on HaCaT keratinocytes. PBS was a blank control. (A) Effect of ULPs on the cell proliferation of HaCaT keratinocytes at 24 h. (B) Effect of different concentrations of ULP15 on the cell proliferation of fibroblast cells at 24 h. (C) HaCaT cell viability after UVB exposure. HaCaT cells were treated by different concentrations of ULP15 for 24 h and exposed to UVB. PBS was a blank control.

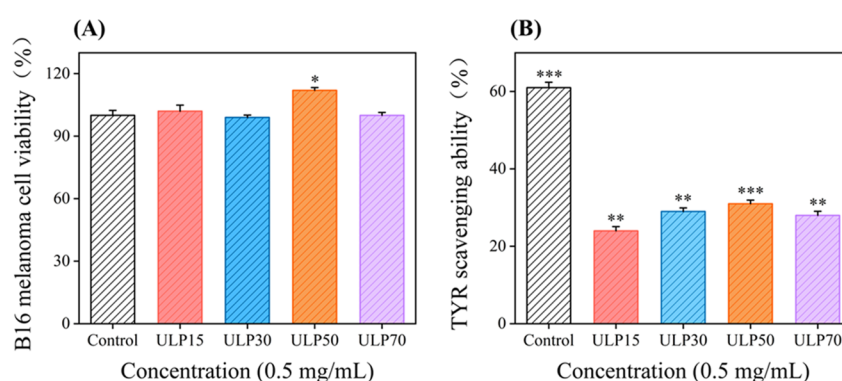


**Figure 7.** (A) Effect of ULPs on the cell proliferation of B16 melanoma cells at 24 h. PBS was a blank control. (B) Inhibitory effects of ULPs on tyrosinase. Ursolic acid was a positive control.

scavenging capacity, followed by ULP70 (53.47%), ULP30 (52.31%), and ULP50 (32.36%) at the concentration of 5 mg/mL. The maximum value of ULP15 was 65.33%, which reached 67.95% that of Vc. The results were similar to the hydroxyl radical scavenging activity of polysaccharides from *Dendrobium officinale*.<sup>34</sup>

According to the results of free radical scavenging ability and reducing ability, the obtained ULPs exhibited antioxidant ability. Considering comprehensively, the antioxidant ability of ULP15 was relatively stronger.

**2.8. Effect of Proliferation on Human HaCaT Keratinocytes and Dermal Fibroblasts.** The proliferative effect of ULPs on HaCaT keratinocytes and dermal fibroblasts was quantified immediately by 3-(4,5-dimethylthiazol-2-yl)-2,5-diphenyltetrazolium bromide (MTT) assay after 24 h treatment. According to Figure 6A, compared with the control group, ULP15, ULP30, and ULP50 had promoted HaCaT keratinocyte growth except for ULP70. Among them, ULP15 had the highest proliferative effect. Given the better proliferative effect on HaCaT keratinocytes, the effect of different concentrations of ULP15 on the proliferation of fibroblasts was investigated. As shown in Figure 6B, ULP15 promoted fibroblast proliferation between the concentrations of 0.01 and 1 mg/mL in a dose-independent manner, a common phenomenon described in the literature for epidermal cell systems.<sup>35</sup> Dose linearity was not found for fibroblasts, which indicated a punctual stimulus, also at low concentrations, initiating signal transduction, leading to an amplification process.<sup>36</sup> A previous study indicated that polysaccharides

could accelerate the proliferation activity of fibroblasts due to their positive effect on the production of glycogen, DNA synthesis, and the formation of collagen in human fibroblasts.<sup>37</sup>

**2.9. UVB-Protective Effects.** UVB irradiation induced the cytotoxic effect on HaCaT keratinocytes mainly by accelerating ROS production. UVB could easily penetrate the stratum corneum and inhibit skin cell growth. To investigate the protective effects of polysaccharides on the skin under UVB irradiation, the protective effect of ULP15 against UVB irradiation-induced proliferation inhibition was studied based on the HaCaT keratinocyte model. As shown in Figure 6C, after UVB irradiation at 40 mJ/cm<sup>2</sup> for 24 h, the viability of the HaCaT keratinocytes was significantly increased by pretreatment with different concentrations of ULP15 compared with the PBS control. Meanwhile, HaCaT keratinocyte viability had a direct connection with the dose of ULP15. When the concentration reached 0.5 mg/mL, cell viability (50%) was significantly higher than that of the control group (61%). In conclusion, ULP15 was able to improve UVB irradiation-induced HaCaT keratinocyte proliferation inhibition, and the recovery effect of the cells was positively associated with the concentration of ULP15, indicating the potential application of ULP15 in anti-UVB cosmetics.

**2.10. Tyrosinase Inhibitory Effects.** The assay of tyrosinase inhibitory effects was carried out based on the B16 murine melanoma cell model. The effect of ULPs with the same concentration of 0.5 mg/mL on the cell proliferation of B16 murine melanoma cells was investigated (Figure 7A). All

ULPs were nontoxic to B16 murine melanoma cells under the examined dose of 0.5 mg/mL.

The biosynthesis reaction of melanin was determined by tyrosinase, and aberrant melanin production could bring about various skin hyperpigmentation disorders.<sup>38</sup> Tyrosinase inhibitory activities of ULPs were tested, and the results are shown in Figure 7B. The maximum tyrosinase inhibition activity was achieved by ULP50 (31%), which was equivalent to half of the positive reference inhibition rate of ursolic acid (61%). Meanwhile, ULP30 and ULP70 showed similar inhibition activity of tyrosinase. The tyrosinase inhibitory ability of ULPs was probably attributed to the hydroxyl groups, which formed hydrogen bonds with the active site of tyrosinase, changed the conformation and steric hindrance of tyrosinase, and influenced the stability of tyrosinase.<sup>39</sup> In addition, considering that tyrosinase also catalyzed the oxidation of 3,4-dihydroxyphenylalanine (L-DOPA) to dopa-quinone, it can be speculated that the antityrosinase ability of ULPs is associated with its antioxidant property.<sup>40</sup> In summary, ULPs showed excellent tyrosinase inhibitory activity that could be used for skin whitening and antioxidants in the cosmetic industry.

### 3. CONCLUSIONS

In this work, four polysaccharide fractions (ULP15, ULP30, ULP50, and ULP70) were successfully obtained from water-soluble polysaccharides of *U. longissima* fractionated via graded ethanol precipitation. ULPs are heteropolysaccharides with a few proteins and uronic acid, and glucose is the major monosaccharide. The ULPs contained hydroxyl, ester, amino, alkyl, and carboxyl. ULPs had no triple-helical conformation and exhibited relative stability below 230 °C. Antioxidant activity assays indicated that the four ULPs all exhibited excellent reducing power and outstanding free radical scavenging capacities on DPPH, ABTS, and hydroxyl in a dose-dependent manner. Among them, ULP15 exhibited the highest antioxidant activity. In the skin protection activity assays, ULP15 had a better proliferative effect on human HaCaT keratinocytes and fibroblast cells. Furthermore, ULP15 exhibited tyrosinase inhibition activity and improved UVB irradiation-induced proliferation inhibition. In summary, ULP15 was of great potential as an active ingredient used in cosmetics. However, the limitation is that only in vitro experiments have been carried out here, and further study can be conducted to explore the relationship between the in vitro activities and their physicochemical properties.

### 4. MATERIALS AND METHODS

**4.1. Materials.** *U. longissima* was collected from Nyingchi, Tibet, China. The collection date was June 2018 in Nyingchi (29°9'14"N 94°12'54"E, 3150 m altitude). A voucher specimen was deposited in the herbarium of the Beijing Forestry University (Beijing, China). All standard chemicals and reagents were of analytical grade and provided by local authorized suppliers.

**4.2. Extraction and Fractionation.** The extraction and fractionation of polysaccharides from *U. longissima* are illustrated in Figure 8. Briefly, *U. longissima* thalli were cleaned and extracted in a Soxhlet apparatus with acetone (solid:liquid = 1:20 g/mL) for 6 h at 75 °C. Then, the defatted solid residue was extracted with distilled water (solid:liquid = 1:20 g/mL) for 6 h at 85 °C; this extraction process was repeated twice.

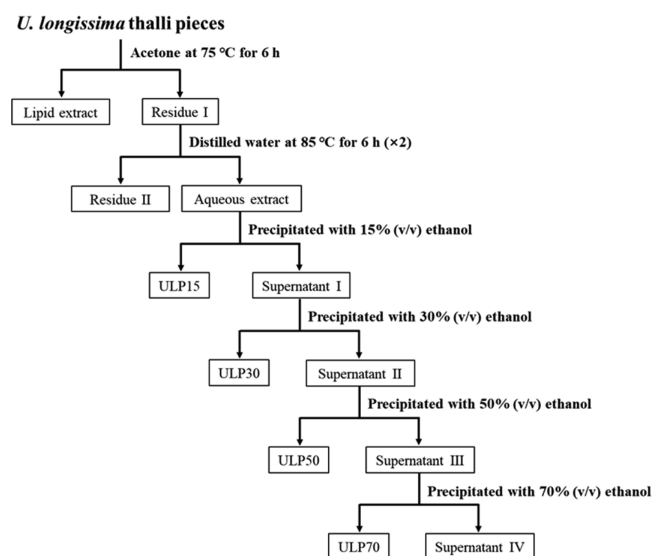


**Figure 8.** Extraction and fractionation procedure of polysaccharide fractions from *U. longissima* thalli.

The obtained aqueous extraction was centrifuged (10,000 rpm, 10 min) and concentrated at reduced pressure to a certain volume.

The concentrated aqueous extraction was precipitated with ethanol (99%, v/v) until the final ethanol concentration was 15% (v/v) and kept in continuous stirring overnight at room temperature. After centrifugation (10,000 rpm, 10 min), the collected precipitate was subjected to dissolution, dialysis, and lyophilization to obtain the first ULP fraction, which was designated as ULP15. Afterward, the remaining supernatant was concentrated at reduced pressure to a certain volume and precipitated with ethanol (99%, v/v) until the final ethanol concentration was 30% (v/v), which was designated as ULP30. Similarly, the two other ULP fractions, namely, ULP50 and ULP70, were obtained by adding ethanol (99%, v/v) into the resultant supernatant until the final ethanol concentration was 50 and 70% (v/v), respectively. The extraction yield of ULPs was determined by the equation

$$\text{yield}(\%) = \frac{W_{\text{ULPs}}}{W_{\text{residue}}} \times 100\% \quad (1)$$

where  $W_{\text{ULPs}}$  represents the dry weight of the polysaccharide powder and  $W_{\text{residue}}$  represents that of the defatted solid residue.

**4.3. Determination of the Physicochemical Properties of ULPs.** The total sugar content was determined by the phenol–sulfuric acid assay with glucose as the standard.<sup>41</sup> The protein content was evaluated by using a total protein quantitative assay kit (Nanjing Jiancheng Bioengineering Institute, China).

The monosaccharide composition of ULPs was determined by high-performance anion exchange chromatography (HPAEC) (Dionex ISC 3000, USA) according to a previous method with minor modifications.<sup>42</sup> Briefly, each polysaccharide sample (4–5 mg) was hydrolyzed at 105 °C for 2.5 h with 10% H<sub>2</sub>SO<sub>4</sub> in the sealed test tube. Next, the hydrolysate was diluted 70-fold, filtered with a 0.22 μm PES (polyethersulfone) filter, and injected into the HPAEC system for analysis. L-Arabinose, D-galactose, D-glucose, D-xylose, D-mannose, and galacturonic and glucuronic acids were used as the standards for calibration and quantification.

The molecular weight and homogeneity of ULPs were analyzed by gel permeation chromatography (GPC) (Agilent 1200, USA) with a differential refractive index detector and PL aqua gel-OH MIXED-M column (300 × 7.5 mm, Agilent Technologies, Inc.). Polysaccharides were dissolved with eluent (20 mM NaCl in 5 mM sodium phosphate buffer, pH 7.5) at a concentration of 2 mg/mL and filtrated through a PES filter, and then 5 μL of the solution was injected into GPC.

The ultraviolet absorbance of the ULP aqueous solution (1 mg/mL) was scanned at room temperature in the wavelength range of 200–600 nm by using a UV spectrophotometer (Techcomp, China). An FT-IR spectrometer (Bruker, Germany) was used to characterize the structure of ULPs.

The TG and DTG analyses of ULPs were performed using a thermal analyzer (Leco, American). The ULPs (5 mg) were introduced into an Al<sub>2</sub>O<sub>3</sub> crucible and heated from 25 to 700 °C with a heating rate of 10 °C/min. Nitrogen was used as the carrier gas at a flow rate of 25 mL/min.

**4.4. Congo Red Test.** The triple-helical structure of ULPs was characterized by the Congo red test.<sup>43</sup> The ULPs (5 mg) were dissolved in 2.0 mL of distilled water and mixed with 2.0 mL of Congo red reagent (80 μmol/L). Different volumes of 1.0 mol/L NaOH solution (0–2.0 mL) were gradually added to maintain the final concentration of the mixture solution in the range of 0–0.5 mol/L. Meanwhile, the same mixture solution without ULPs was used as the control. A UV spectrophotometer was used to measure the λ<sub>max</sub> under each alkaline condition in the range from 200 to 800 nm after equilibrating for 5 min at room temperature.

**4.5. Antioxidant Activity.** The free radical scavenging ability of ULPs was evaluated by the stable DPPH, following the reported method.<sup>44</sup> The ABTS radical scavenging ability of ULPs was measured according to the instruction by the Beyotime Institute of Biotechnology (Beyotime Biotechnology, China). Hydroxyl radical scavenging activities of ULPs were performed according to the reported method.<sup>45</sup> All assays were repeated three times, and Vc was used as the positive control. The DPPH, ABTS, and hydroxyl free radical scavenging activities (%) were calculated using the following equations:

$$\begin{aligned} &\text{DPPH radical scavenging activity (\%)} \\ &= [1 - (A_1 - A_2)/A_0] \times 100\% \end{aligned} \quad (2)$$

$$\begin{aligned} &\text{ABTS radical cation scavenging activity (\%)} \\ &= (1 - A_3/A_4) \times 100\% \end{aligned} \quad (3)$$

$$\begin{aligned} &\text{hydroxyl radical scavenging activity (\%)} \\ &= [1 - (A_5/A_6)/A_7] \times 100\% \end{aligned} \quad (4)$$

where A<sub>0</sub> means the absorption of the blank (DPPH solution without the sample), A<sub>1</sub> means the absorption of the sample mixture, A<sub>2</sub> means the absorption of the sample solution without DPPH, A<sub>3</sub> means the absorbance of the control (ABTS solution without the test sample), A<sub>4</sub> means the absorbance of the polysaccharide samples, A<sub>5</sub> means the absorption of the sample mixture, A<sub>6</sub> means the background absorption (water instead of H<sub>2</sub>O<sub>2</sub>), and A<sub>7</sub> means the absorption of the blank (distilled water instead of the sample).

The reducing power of ULPs was determined by the potassium ferricyanide method.<sup>45</sup>

#### 4.6. Cell Culture and Cell Proliferative Effect Assay.

Human HaCaT keratinocytes, dermal fibroblasts, and B16 murine melanoma cells were cultured and maintained in minimum essential medium (MEM) (Gibco, USA). The cultures were incubated at 37 °C in a 5% CO<sub>2</sub> incubator.

HaCaT keratinocytes and dermal fibroblasts were plated in 96-well plates (1.2 × 10<sup>4</sup> cells/well). Different concentrations of samples were added with serum-free MEM and incubated for 24 h. The proliferative effects of ULPs on the cells were analyzed by the reported MTT assay.<sup>46</sup> Similarly, the B16 murine melanoma cells were seeded into a 96-well plate (5 × 10<sup>3</sup> cells/well). After 24 h of incubation, 0.5 mg/mL ULPs were added to each well. Cell viability was determined using the previously mentioned MTT assay. The cell proliferation rate of the blank control group was set as 100%. If the proliferation rate was more than 100%, then the tested sample accelerated cell proliferation; if not, it suppressed cell proliferation. All experiments were repeated at least three times.

**4.7. UVB-Protective Effects.** HaCaT keratinocytes were seeded into a 96-well plate (5 × 10<sup>3</sup> cells/well) and cultured for 72 h at 37 °C in a 5% CO<sub>2</sub> incubator. Samples of ULP15 with different concentrations (0.05, 0.1, 0.2, and 0.5 mg/mL) were added in wells and incubated for 24 h. Next, the substrate in each well was changed to PBS (phosphate-buffered solution) (pH 7.2) and exposed to 40 mJ/cm<sup>-2</sup> of UVB radiation (312 nm) using a Bio-Sun ultraviolet irradiator (Vilber Lourmat, France). The culture medium without a sample was used as a control. After the irradiation, PBS was immediately withdrawn from the wells and replaced with MEM containing various concentrations of ULP15 and FBS (fetal bovine serum) (10%, v/v). Cell viability was determined using the previously mentioned MTT assay.

**4.8. Tyrosinase Inhibitory Assays.** The tyrosinase inhibitory activity of ULPs was measured based on L-DOPA oxidase activity according to the method described previously.<sup>40</sup> The B16 murine melanoma cells were seeded into a 96-well plate (1 × 10<sup>5</sup> cells/well), and then the prepared polysaccharide solution (0.5 mg/mL) was added and incubated for 48 h. Subsequently, the substrate solution was removed and the cells were washed twice with PBS solution (200 μL, pH 7.2). Next, the cells were immediately lysed using 100 μL of Triton X-100 (1%, v/v) in the freezer (−80 °C) for 30 min. Fifty microliters of L-DOPA (0.2%, m/m) was added to each well at room temperature after 30 min. This mixture was incubated for 3 h at 37 °C, and the absorbance was measured at 490 nm by using a microplate reader (BioTek, USA). Ursolic acid was used as a positive control. Tyrosinase inhibitory activity was calculated using the following formula

$$\text{inhibitory activity} = (1 - \text{OD}_{\text{sample}}/\text{OD}_{\text{control}}) \times 100\% \quad (5)$$

**4.9. Statistical Analysis.** The results of the experiments were recorded as means ± standard deviations (SD). SPSS software (version 11.0 for Windows, SPSS Inc., Chicago, IL, USA) was used for statistical analysis. \*P < 0.05, \*\*P < 0.01, and \*\*\*P < 0.001 were considered significantly different.

## ■ AUTHOR INFORMATION

### Corresponding Author

Feng Peng – Beijing Key Laboratory of Lignocellulosic Chemistry, Beijing Forestry University, Beijing 100083,



China;  [orcid.org/0000-0003-0266-5869](https://orcid.org/0000-0003-0266-5869);  
Phone: 15811052459; Email: [fengpeng@bjfu.edu.cn](mailto:fengpeng@bjfu.edu.cn)

## Authors

**Ziying Yang** – Beijing Key Laboratory of Lignocellulosic Chemistry, Beijing Forestry University, Beijing 100083, China

**Yajie Hu** – Beijing Key Laboratory of Lignocellulosic Chemistry, Beijing Forestry University, Beijing 100083, China

**Panpan Yue** – Beijing Key Laboratory of Lignocellulosic Chemistry, Beijing Forestry University, Beijing 100083, China

**Hongdan Luo** – Department of Dermatology, Zunyi Hospital of Traditional Chinese Medicine, Zunyi, Guizhou 563000, China

**Qisui Li** – Meteorological Bureau of Meishan City, Meishan, Sichuan 620010, China

**Huilong Li** – JALA Research Center, JALA Group Co. Ltd., Shanghai 200233, China

**Zhang Zhang** – JALA Research Center, JALA Group Co. Ltd., Shanghai 200233, China

Complete contact information is available at:  
<https://pubs.acs.org/10.1021/acsoomega.1c04163>

## Author Contributions

<sup>†</sup>Z.Y. and Y.H. contributed equally to this study as co-first authors.

## Notes

The authors declare no competing financial interest.

## ACKNOWLEDGMENTS

This work was supported by the Beijing Forestry University Outstanding Young Talent Cultivation Project (2019JQ03017), JALA Corporation (YF-ZX-201803-0320), and Ministry of Education, China-111 Project (BP0820033).

## REFERENCES

- (1) Wang, L.; Kim, H. S.; Oh, J. Y.; Je, J. G.; Jeon, Y.-J.; Ryu, B. Protective effect of diphlorethohydroxycarmalol isolated from *Ishige okamurae* against UVB-induced damage *in vitro* in human dermal fibroblasts and *in vivo* in zebrafish. *Food Chem. Toxicol.* **2020**, *136*, 110963.
- (2) Seo, S.-Y.; Sharma, V. K.; Sharma, N. Mushroom tyrosinase: recent prospects. *J. Agr. Food Chem.* **2003**, *51*, 2837–2853.
- (3) Jesumani, V.; Du, H.; Pei, P.; Zheng, C.; Cheong, K.-L.; Huang, N. Unravelling property of polysaccharides from *Sargassum* sp. as an anti-wrinkle and skin whitening property. *Int. J. Biol. Macromol.* **2019**, *140*, 216–224.
- (4) Pratoomthai, B.; Songtavisin, T.; Gangnonngiw, W.; Wongprasert, K. *In vitro* inhibitory effect of sulfated galactans isolated from red alga *Gracilaria fisheri* on melanogenesis in B16F10 melanoma cells. *J. Appl. Physiol.* **2018**, *30*, 2611–2618.
- (5) Yu, Y.; Shen, M.; Song, Q.; Xie, J. Biological activities and pharmaceutical applications of polysaccharide from natural resources: A review. *Carbohydr. Polym.* **2018**, *183*, 91–101.
- (6) Kim, I.-S.; Yoon, S.-J.; Park, Y.-J.; Lee, H.-B. Inhibitory effect of ephedranins A and B from roots of *Ephedra sinica* STAPF on melanogenesis. *Biochim. Biophys. Acta* **2015**, *1850*, 1389–1396.
- (7) Fernando, I. P. S.; Dias, M. K. M. H.; Madusanka, D. M. D.; Han, E. J.; Kim, M. J.; Jeon, Y.-J.; Ahn, G. Step gradient alcohol precipitation for the purification of low molecular weight fucoidan from *Sargassum siliquastrum* and its UVB protective effects. *Int. J. Biol. Macromol.* **2020**, *163*, 26–35.

(8) Yuan, L.; Duan, X.; Zhang, R.; Zhang, Y.; Qu, M. Aloe polysaccharide protects skin cells from UVB irradiation through Keap1/Nrf2/ARE signal pathway. *J. Dermatol. Treat.* **2020**, *31*, 300–308.

(9) Chou, C.-H.; Sung, T.-J.; Hu, Y.-N.; Lu, H.-Y.; Yang, L.-C.; Cheng, K.-C.; Lai, P.-S.; Hsieh, C.-W. Chemical analysis, moisture-preserving, and antioxidant activities of polysaccharides from *Pholiota nameko* by fractional precipitation. *Int. J. Biol. Macromol.* **2019**, *131*, 1021–1031.

(10) Tuong, T. L.; Do, L. T. M.; Aree, T.; Wonganan, P.; Chavasiri, W. Tetrahydroxanthone-chromanone heterodimers from lichen *Usnea aciculifera* and their cytotoxic activity against human cancer cell lines. *Fitoterapia* **2020**, *147*, 104732.

(11) Olafsdottir, E. S.; Ingólfssdottir, K. Polysaccharides from lichens: structural characteristics and biological activity. *Planta Med.* **2001**, *67*, 199–208.

(12) Shrestha, G.; St. Clair, L. L.; O'Neill, K. L. The immunostimulating role of lichen polysaccharides: A review. *Phytother. Res.* **2015**, *29*, 317–322.

(13) Ullah, M.; Uddin, Z.; Song, Y. H.; Li, Z. P.; Kim, J. Y.; Ban, Y. J.; Park, K. H. Bacterial neuraminidase inhibition by phenolic compounds from *Usnea longissima*. *S. Afr. J. Bot.* **2019**, *120*, 326–330.

(14) Jesumani, V.; Du, H.; Pei, P.; Aslam, M.; Huang, N. Comparative study on skin protection activity of polyphenol-rich extract and polysaccharide-rich extract from *Sargassum vachellianum*. *PLoS One* **2020**, *15*, No. e0227308.

(15) Wu, M.; Li, W.; Zhang, Y.; Shi, L.; Xu, Z.; Xia, W.; Zhang, W. Structure characteristics, hypoglycemic and immunomodulatory activities of pectic polysaccharides from *Rosa setata* x *Rosa rugosa* waste. *Carbohydr. Polym.* **2021**, *253*, 117190.

(16) Wei, X.; Liu, Y.; Xiao, J.; Wang, Y. Protective effects of tea polysaccharides and polyphenols on skin. *J. Agric. Food Chem.* **2009**, *57*, 7757–7762.

(17) Zhang, Z.; Guo, L.; Yan, A.; Feng, L.; Wan, Y. Fractionation, structure and conformation characterization of polysaccharides from *Anoetochilus roxburghii*. *Carbohydr. Polym.* **2020**, *231*, 115688.

(18) Košť'álová, Z.; Hromádková, Z. Structural characterisation of polysaccharides from roasted hazelnut skins. *Food Chem.* **2019**, *286*, 179–184.

(19) Gong, G.; Dang, T.; Deng, Y.; Han, J.; Zou, Z.; Jing, S.; Zhang, Y.; Liu, Q.; Huang, L.; Wang, Z. Physicochemical properties and biological activities of polysaccharides from *Lycium barbarum* prepared by fractional precipitation. *Int. J. Biol. Macromol.* **2018**, *109*, 611–618.

(20) Gao, X.; Qi, J.; Ho, C.-T.; Li, B.; Mu, J.; Zhang, Y.; Hu, H.; Mo, W.; Chen, Z.; Xie, Y. Structural characterization and immunomodulatory activity of a water-soluble polysaccharide from *Ganoderma leucocontextum* fruiting bodies. *Carbohydr. Polym.* **2020**, *249*, 116874.

(21) Muhidinov, Z. K.; Bobokalonov, Z. T.; Ismoilov, I. B.; Strahan, G. D.; Chau, H. K.; Hotchkiss, A. T.; Liu, L. Characterization of two types of polysaccharides from *Eremurus hissaricus* roots growing in Tajikistan. *Food Hydrocolloids* **2020**, *105*, 105768.

(22) Zhang, H.; Zou, P.; Zhao, H.; Qiu, J.; Regenstein, J. M.; Yang, X. Isolation, purification, structure and antioxidant activity of polysaccharide from pinecones of *Pinus koraiensis*. *Carbohydr. Polym.* **2021**, *251*, 117078.

(23) Jiang, L.; Wang, W.; Wen, P.; Shen, M.; Li, H.; Ren, Y.; Xiao, Y.; Song, Q.; Chen, Y.; Yu, Q.; Xie, J. Two water-soluble polysaccharides from mung bean skin: physicochemical characterization, antioxidant and antibacterial activities. *Food Hydrocolloids* **2020**, *100*, 105412.

(24) Chen, Y.-y.; Xue, Y.-t. Optimization of microwave assisted extraction, chemical characterization and antitumor activities of polysaccharides from *porphyra haitanensis*. *Carbohydr. Polym.* **2019**, *206*, 179–186.

(25) Kim, S.-S.; Ly, H. V.; Kim, J.; Choi, J. H.; Woo, H. C. Thermogravimetric characteristics and pyrolysis kinetics of alga *Sargassum* sp. biomass. *Bioresour. Technol.* **2013**, *139*, 242–248.



- (26) Zhi, F.; Yang, T.-L.; Wang, Q.; Jiang, B.; Wang, Z.-P.; Zhang, J.; Chen, Y.-Z. Isolation, structure and activity of a novel water-soluble polysaccharide from *Dioscorea opposita* Thunb. *Int. J. Biol. Macromol.* **2019**, *133*, 1201–1209.
- (27) Leong, L. P.; Shui, G. An investigation of antioxidant capacity of fruits in Singapore markets. *Food Chem.* **2002**, *76*, 69–75.
- (28) Re, R.; Pellegrini, N.; Proteggente, A.; Pannala, A.; Yang, M.; Rice-Evans, C. Antioxidant activity applying an improved ABTS radical cation decolorization assay. *Free Radical Biol. Med.* **1999**, *26*, 1231–1237.
- (29) Yan, J.-K.; Wu, L.-X.; Qiao, Z.-R.; Cai, W.-D.; Ma, H. Effect of different drying methods on the product quality and bioactive polysaccharides of bitter melon (*Momordica charantia* L.) slices. *Food Chem.* **2019**, *271*, 588–596.
- (30) Mukai, K.; Ouchi, A.; Azuma, N.; Takahashi, S.; Aizawa, K.; Nagaoka, S.-i. Development of a Singlet Oxygen Absorption Capacity (SOAC) Assay Method. Measurements of the SOAC Values for Carotenoids and  $\alpha$ -Tocopherol in an Aqueous Triton X-100 Micellar Solution. *J. Agric. Food Chem.* **2017**, *65*, 784–792.
- (31) Ouchi, A.; Aizawa, K.; Iwasaki, Y.; Inakuma, T.; Terao, J.; Nagaoka, S.; Mukai, K. Kinetic study of the quenching reaction of singlet oxygen by carotenoids and food extracts in solution. Development of a singlet oxygen absorption capacity (SOAC) assay method. *J. Agric. Food Chem.* **2010**, *58*, 9967–9978.
- (32) Gulcin, I. Antioxidants and antioxidant methods: an updated overview. *Arch. Toxicol.* **2020**, *94*, 651–715.
- (33) Phaniendra, A.; Jestadi, D. B.; Periyasamy, L. Free radicals: properties, sources, targets, and their implication in various diseases. *Indian J. Clin. Biochem.* **2015**, *30*, 11–26.
- (34) Xing, S.; Zhang, X.; Ke, H.; Lin, J.; Huang, Y.; Wei, G. Physicochemical properties of polysaccharides from *Dendrobium officinale* by fractional precipitation and their preliminary antioxidant and anti-HepG2 cells activities in vitro. *Chem. Cent. J.* **2018**, *12*, 100.
- (35) Cai, C.; Guo, Z.; Yang, Y.; Geng, Z.; Tang, L.; Zhao, M.; Qiu, Y.; Chen, Y.; He, P. Inhibition of hydrogen peroxide induced injuring on human skin fibroblast by *Ulva prolifera* polysaccharide. *Int. J. Biol. Macromol.* **2016**, *91*, 241–247.
- (36) Deters, A. M.; Schröder, K. R.; Hensel, A. Kiwi fruit (*Actinidia chinensis* L.) polysaccharides exert stimulating effects on cell proliferation via enhanced growth factor receptors, energy production, and collagen synthesis of human keratinocytes, fibroblasts, and skin equivalents. *J. Cell. Physiol.* **2005**, *202*, 717–722.
- (37) Yao, H.; Chen, Y.; Li, S.; Huang, L.; Chen, W.; Lin, X. Promotion proliferation effect of a polysaccharide from *Aloe barbadensis* Miller on human fibroblasts in vitro. *Int. J. Biol. Macromol.* **2009**, *45*, 152–156.
- (38) Hemachandran, H.; Jain, F.; Mohan, S.; Kumar, D. T.; Priya Doss, C. G.; Ramamoorthy, S. Glandular hair constituents of *Mallotus philippinensis* Muell. fruit act as tyrosinase inhibitors: Insights from enzyme kinetics and simulation study. *Int. J. Biol. Macromol.* **2018**, *107*, 1675–1682.
- (39) Song, K.-K.; Huang, H.; Han, P.; Zhang, C.-L.; Shi, Y.; Chen, Q.-X. Inhibitory effects of *cis*- and *trans*-isomers of 3,5-dihydroxystilbene on the activity of mushroom tyrosinase. *Biochem. Biophys. Res. Commun.* **2006**, *342*, 1147–1151.
- (40) Chen, B.-J.; Shi, M.-J.; Cui, S.; Hao, S.-X.; Hider, R. C.; Zhou, T. Improved antioxidant and anti-tyrosinase activity of polysaccharide from *Sargassum fusiforme* by degradation. *Int. J. Biol. Macromol.* **2016**, *92*, 715–722.
- (41) DuBois, M.; Gilles, K. A.; Hamilton, J. K.; Rebers, P. A.; Smith, F. Colorimetric method for determination of sugars and related substances. *Anal. Chem.* **1956**, *28*, 350–356.
- (42) Peng, F.; Ren, J.-L.; Xu, F.; Bian, J.; Peng, P.; Sun, R.-C. Fractional study of alkali-soluble hemicelluloses obtained by graded ethanol precipitation from sugar cane bagasse. *J. Agr. Food Chem.* **2010**, *58*, 1768–1776.
- (43) Zhu, Z.-Y.; Luo, Y.; Dong, G.-L.; Ren, Y.-Y.; Chen, L.-J.; Guo, M.-Z.; Wang, X.-T.; Yang, X.-Y.; Zhang, Y. Effects of the ultra-high pressure on structure and  $\alpha$ -glucosidase inhibition of polysaccharide from *Astragalus*. *Int. J. Biol. Macromol.* **2016**, *87*, 570–576.
- (44) Xu, D.; Wang, C.; Zhuo, Z.; Ye, M.; Pu, B. Extraction, purification and antioxidant activity of polysaccharide from cold pressed oil cake of 'Tengjiao' seed. *Int. J. Biol. Macromol.* **2020**, *163*, 508–518.
- (45) Li, J.-E.; Wang, W.-J.; Zheng, G.-D.; Li, L.-Y. Physicochemical properties and antioxidant activities of polysaccharides from *Gynura procumbens* leaves by fractional precipitation. *Int. J. Biol. Macromol.* **2017**, *95*, 719–724.
- (46) Kao, C.-J.; Chou, H.-Y.; Lin, Y.-C.; Liu, Q.; David Wang, H.-M. Functional analysis of macromolecular polysaccharides: whitening, moisturizing, anti-oxidant, and cell proliferation. *Antioxidants* **2019**, *8*, 533.